Bond-order–bond-length–bond-strength (bond-OLS) correlation mechanism for the shape-and-size dependence of a nanosolid

2002 J. Phys.: Condens. Matter 14 7781

(http://iopscience.iop.org/0953-8984/14/34/301)

INSTITUTE OF PHYSICS PUBLISHING JOURNAL OF PHYSICS: CONDENSED MATTER

J. Phys.: Condens. Matter **14** (2002) 7781–7795 PII: S0953-8984(02)35620-0

Bond-order–bond-length–bond-strength (bond-OLS) correlation mechanism for the shape-and-size dependence of a nanosolid

Chang Q Sun[1,2,5], B K Tay[1], X T Zeng[3], S Li[1], T P Chen[1], Ji Zhou[4], H L Bai[2] and E Y Jiang[2]

[1] School of Electrical and Electronic Engineering, Nanyang Technological University, 639798, Singapore
[2] Institute of Advanced Materials Physics and Faculty of Science, Tianjin University, Tianjin 300072, People's Republic of China
[3] Singapore Institute of Manufacturing Technology, 637875, Singapore
[4] State Key Laboratory of New Ceramics and Fine Processing, Tsinghua University, Beijing 100084, People's Republic of China

E-mail: ecqsun@ntu.edu.sg

Received 8 April 2002
Published 15 August 2002
Online at stacks.iop.org/JPhysCM/14/7781

Abstract

A bond-order–bond-length–bond-strength (bond-OLS) correlation mechanism is presented for consistent insight into the origin of the shape-and-size dependence of a nanosolid, aiming to provide guidelines for designing nanomaterials with desired functions. It is proposed that the coordination number imperfection of an atom at a surface causes the remaining bonds of the lower-coordinated surface atom to relax spontaneously; as such, the bond energy rises (in absolute value). The bond energy rise contributes not only to the cohesive energy (E_{Coh}) of the surface atom but also to the energy density in the relaxed region. E_{Coh} relates to thermodynamic properties such as self-assembly, phase transition and thermal stability of a nanosolid. The binding energy density rise is responsible for the changes of the system Hamiltonian and related properties, such as the bandgap, core-level shift, phonon frequency and the dielectrics of a nanosolid of which the surface curvature and the portion of surface atoms vary with particle size. The bond-OLS premise, involving no assumptions or freely adjustable parameters, has led to consistency between predictions and experimental observations of a number of outstanding properties of nanosolids.

(Some figures in this article are in colour only in the electronic version)

[5] http://www.ntu.edu.sg/home/ecqsun/

1. Introduction

With miniaturization of a solid down to nanometre scale, quantum and interfacial effects become dominant. Such effects have led to amazing changes of many properties of a single nanosolid and its assemblies, which forms the base of nanoscience and nanotechnology. The classical characteristics of a solid, such as the surface stress, Young's modulus, phonon frequency, specific heat, critical temperatures for melting, phase transition or evaporation, energy bandgap, core-level shift and dielectric constant as well as the saturation magnetization, are all no longer constant but they are tunable by simply controlling the shape and size of the physical system. Such a freedom of property change has been leading to a revolution in materials science and device technology. However, the origin, the trends and the amplitudes of the size-related changes are still far from clear; for instance, conflicting models such as quantum confinement [1], surface stress [2], surface states [3] and impurity centres [4] have been frequently referred to for a certain specific phenomenon such as the blue-shift in the photoluminescence of nanometric semiconductors. Here we present a simple mechanism, free from assumptions or freely adjustable parameters, aiming to unify as far as possible the changes caused by changing the shape and size of the physical system and to provide guidelines for designing nanomaterials with desired functions.

2. Model

2.1. Principles

2.1.1. Bond-order–bond-length–bond-strength correlation mechanism. The termination of the lattice periodicity in the surface normal has two consequences. First, the imperfection of the coordination numbers (CNs) of a surface atom causes the lengths of the remaining bonds of this lower-coordinated surface atom to relax [5, 6]. As the relaxation (both contraction and expansion) is a spontaneous process, the binding energy of the relaxed bond will reduce (rise in absolute value) to minimize the system energy. The relaxed bond is also stronger. Such a bond-order–bond-length–bond-strength (bond-OLS) correlation premise has been recognized as the force that drives the O–Cu(001) surface to reconstruct, and the O–Cu bond to contract by 4–12%, that forms one of the four discrete stages of the Cu_3O_2 bonding kinetics at the O–Cu(001) surface [7, 8]. It is important to note that the bond relaxation is independent of the nature of the specific chemical bond [9] or the dimension of the solid [10] though the extent of relaxation may vary from situation to situation (see samples in table 1).

The CN-imperfection-induced bond relaxation can be defined as $d_i = c_i d$ by introducing a coefficient $c_i < 1$ for bond contraction and $c_i > 1$ for bond expansion. As listed in table 1, most of the bonds contract, which has an enormous effect on the properties of a surface. Bond expansion might happen but the system energy must be minimized, unless the relaxation is a process proceeding under external stimulus such as heating or pressure. The bond contraction and the response of bond energy can be expressed as

$$\begin{aligned} &\frac{\Delta d_i}{d} = c_i - 1 < 0; \\ &\frac{\Delta E_B(d_i)}{E_B(d)} = \frac{E_B(d_i)}{E_B(d)} - 1 = c_i^{-m} - 1 > 0. \end{aligned} \tag{1}$$

Subscript i denotes the ith atomic layer, which may be counted up to three from the outermost atomic layer to the centre of the solid as no CN reduction is expected for $i > 3$. m describes the bond-length dependence of the binding-energy change, $E_B(d_i) = c_i^{-m} E_B(d)$, at equilibrium atomic separation. d and $E_B(d)$ are the corresponding bulk values. c_i^{-m} is independent of

Table 1. Bond length relaxation for typical covalent, metallic and ionic solids and its effect on the physical properties of the corresponding solid or surface, where d and d_1 are the bond lengths for atoms inside the bulk and for atoms at the surface, respectively. c_1 is the bond contraction coefficient, that varies from source to source.

Bond nature	Medium	$c_1 = d_1/d$	Effect
Covalent	Diamond {111} [11]	0.7	Surface energy decrease
Metallic	Ru [12] Co [13] and	0.9	
	Re [14] $(10\bar{1}0)$ surfaces	0.9	Atomic magnetic momentum
	Fe–W, Fe–Fe [15]	0.88	is increased by (25–27)%
	Fe(310) [16], N(210) [17]	0.88	[15–17]
	Al(001) [18]		Cohesive energy rises by
	Ni, Cu, Ag, Au, Pt and	0.85–0.9	0.3 eV/bond [18].
	Pd dimer bond [19]		Single-bond energy increases
	Ti, Zr [20]	0.7	2–3-fold [19]
	V [20]	0.6	
Ionic	O–Cu(001) [8, 21]	0.88–0.96	
	O–Cu(110) [8]	0.9	N–TiCr surface is 100%
	N–Tr/Cr [22]	0.86–0.88	harder that the bulk [22].
Extraordinary	(Be, Mg) (0001) Zn, Cd	>1	No indication of effects on
cases	and Hg dimer bond [20]		physical properties is yet given.

the types of interatomic potential. Exercises so far [23–25] revealed that for elemental solids, $m \approx 1$; for compounds and alloys, $m \approx 4$.

Figure 1 illustrates the bond-OLS correlation mechanism, showing that the bond becomes shorter and stronger if the effective CN (z_i) decreases. The solid curve in panel (a) formulates the CN (z_i) dependence of the bond length, $c_i(z_i)$, based on the Goldschmidt premise [6] which states that an ionic radius contracts by 12, 4 and 3% if the CN of the atom reduces from 12 to four, six and eight, respectively. Feibelman [20] has noted a 30% contraction of the metallic dimer bond length of Ti, Zr and a 40% contraction of the dimer bond length of V, which is also in line with the formulation. The function $c_i(z_i)$ is so established that it fits the observations [6, 20] aiming to reduce the number of freely adjustable parameters. The bond-OLS correlation can be formulated as [23]

$$\begin{aligned} d_i &= c_i d \\ E_B(d_i) &= c_i^{-m} E_B(d) \\ c_i(z_i) &= \frac{2}{1+\exp[(12-z_i)/8z_i]}. \end{aligned} \tag{2}$$

The bond-OLS premise does not apply to the so-called dangling bond, as a dangling bond is not a real bond forming between two neighbouring atoms. It is true that the concept of localized bond is not applicable to metallic systems due to the delocalized valence electrons whose wavefunction often extends to the entire solid. However, the delocalized valence electrons are often treated as a Fermi sea inside which the metal ions are arranged regularly. As a standard practice [26], the metallic bond length corresponds to the equilibrium atomic separation and the bond energy is defined as the division of the atomic E_{Coh} by the CN in a real system. Therefore, the bond-OLS premise holds for any solid disregarding the nature of the specific chemical bond. The pair-wise potential for metallic interatomic interaction also holds, as the pair-wise potential represents the resultant effect of various orders of coordination and the charge-density distribution. Most strikingly, recent density functional calculations [19] revealed that the dimer bond of Ni, Cu, Ag, Au, Pt and Pd contracts by 10–15% in the single atomic chain compared with the corresponding fcc bulk values. Meanwhile, E_{Coh} per bond

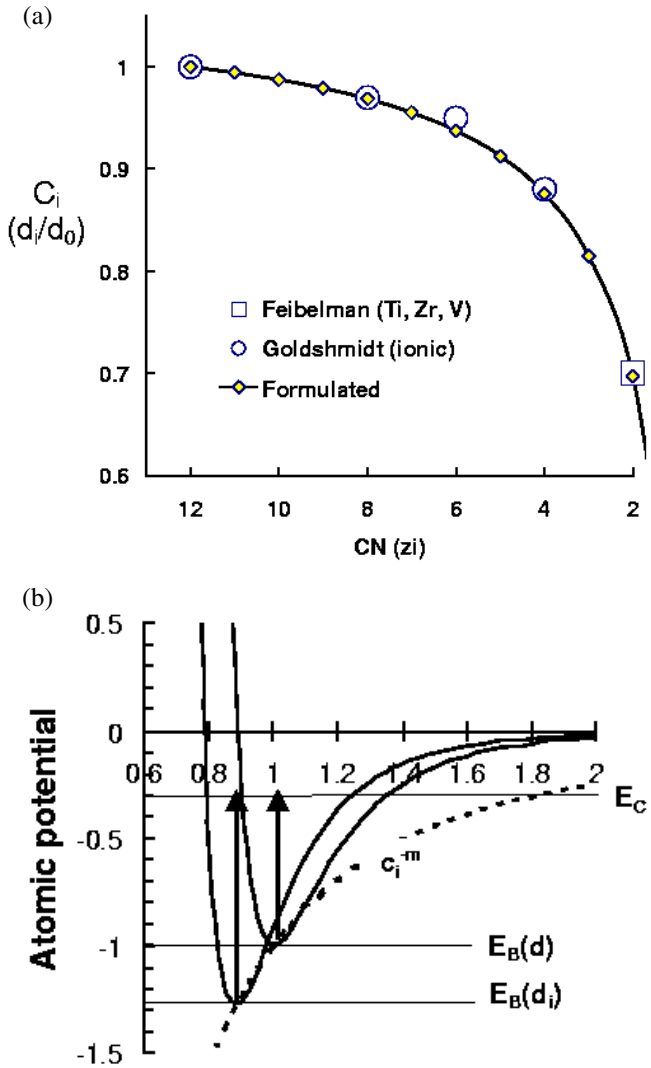

Figure 1. Illustration of the bond-OLS correlation mechanism [25]. The solid curve $c_i(z_i)$ is derived based on the premise of Goldshmidt (open circles) [6] and findings of Feibelman (open square) [20]. As a spontaneous process of bond contraction, the bond energy at equilibrium atomic separation will rise in absolute energy. That is, $E_B(d_i) = c_i^{-m} E_B(d)$. c_i is the contraction factor and m a parameter that varies with the nature of bond. For elemental solids, $m \approx 1$; for compounds, $m \approx 4$ [25, 26].

increases two- to threefold when the single atomic chain forms. This finding not only concurs with the current bond-OLS correlation mechanism but also evidences the validity of the bond-OLS premise for metallic systems.

2.1.2. Barrier confinement—quantum uncertainty. Termination of the lattice periodicity creates the work function, $\varphi(=E_0 - E_F(n^{2/3}))$, that depends merely on the electronic density (n) at the surface. E_0 and E_F are the vacuum energy and the Fermi level, respectively. The surface charge density is modified by the surface chemical states [28]. For instance, the work

function of a metal surface can be reduced by ∼1.2 eV through oxidation, that produces metal dipoles at the surface [27]. The reduced work function can also be recovered when a hydrogen-like bonds form at the surface.

The termination of a lattice also generates a barrier of potential energy to the surface. The potential barrier [28] does not contribute to the system's energy. It should be noted that the barrier has no influence on the strongly localized valence electrons or the bonding electron pairs inside a compound. The barrier only confines the nearly free conduction electrons moving inside metals. However, the barrier confinement is subject to the quantum uncertainty principle. The quantum uncertainty principle indicates that reducing the dimension of a space (D, such as the diameter of a spherical dot), inside which an energetic particle moves, increases the fluctuation, Δp, rather than the mean value, $\overline{p}$, of the momentum ($D \times \Delta p = \hbar$) or the kinetic energy ($E = \overline{p}^2/2\mu$) of the energetic particle with effective mass μ. $\hbar$ is the Planck constant. Therefore, being subject to quantum uncertainty, barrier confinement does not contribute to the system energy no matter what the bond nature involved in the nanosolid.

2.1.3. Surface versus nanosolid. For a solid of nanometre scale, the surface curvature and the portion of surface atoms increase with decreasing particle size. Therefore, the effect of CN imperfection will be more significant with reducing solid size. It is easy to derive the volume or number ratio of a certain atomic layer, denoted i, to that of the entire solid as

$$\gamma_i = \frac{N_i}{N} = \frac{V_i}{V} = \frac{\tau[k-(i-0.5)]^{\tau-1}}{k^\tau - L^\tau} c_i = \gamma_{i0} c_i \leqslant 1, \tag{3}$$

where $D = (2k+1)d$ and k is the number of atoms arranged along the radius of a spherical dot or a rod with $N-1$ atoms surrounding one in the centre. D is also the thickness of a thin plate. τ is the dimensionality of a thin plate ($\tau = 1$), a rod ($\tau = 2$) and a spherical dot ($\tau = 3$) nanometers across. L is the number of atomic layers not occupied by atoms. For a solid system, $L = 0$; while for a hollow sphere or a hollow tube, $L < k$. For a hollow system, the γ_i should count both external and internal sides of the hollow system. With reducing particle size, the performance of surface atoms will dominate because at the smallest size ($k < 3$) γ_1 approaches unity.

2.2. Numerical expressions

Generally, the mean relative change of a traditional quantity Q of a nanosolid containing N atoms, with dimension D, can be expressed as $Q(D)$, and as $Q(\infty)$ for the same solid without considering the effect of surface relaxation. $Q(D)$ relates to $Q(\infty) = Nq$ as follows:

$$Q(D) = (N - N_s)q + N_s q_s = Nq + N_s(q_s - q). \tag{4}$$

q and q_s correspond to the density of Q inside the bulk and in the surface region, respectively. $N_s = \sum N_i$ is the number of atoms in the surface atomic shells. Equation (4) leads to the immediate relation

$$\frac{\Delta Q(D)}{Q(\infty)} = \frac{Q(D) - Q(\infty)}{Q(\infty)} = \frac{N_s}{N}\left(\frac{q_s}{q} - 1\right) = \frac{\sum_{i\leqslant 3} N_i(q_i - q)}{Nq} = \sum_{i\leqslant 3} \gamma_i(q_i/q - 1)$$
$$= \sum_{i\leqslant 3} \gamma_i(\Delta q_i/q). \tag{5}$$

The weighting factor, γ_i, is the surface-to-volume ratio (see equation (3)) that changes with the dimension (k) and dimensionality (τ) of the solid.

Equation (5) represents that the size-and-shape dependence of a detectable quantity for a nanosolid is composed of two essential parts. One is the origin, $\Delta q_i/q$, that determines the sign and amplitude of change; and the other is the weighting factor, γ_i, that determines the trend of change. It is worth noting that $\Delta Q(D)/Q(\infty)$ converges at any size as γ_i is no larger than unity and the relative change of $\Delta q/q$ is always finite.

Physical quintiles of a solid can normally be categorized as follows.

(i) Quantities relating directly to bond length, such as the mean lattice constant, atomic density and binding energy.
(ii) Quantities relating to the atomic cohesive energy, $E_{Coh} = zE_B$, such as the self-organization growth, phase stability, Coulomb blockade and critical temperature for liquidation, evaporation and phase transition of a nanosolid [29].
(iii) Properties relating to the binding energy density in the relaxed region, $q = v(d_i)$. $v(d_i)$ is proportional to the single bond energy $E_B(d_i)$ because the number of bonds per circumferential area between neighbouring atomic layers in the relaxed region does not change. The energy density contributes to the Hamiltonian that determines the entire band structure and related properties such as bandgap, core level, magnetization, phonon frequency, Young's modulus, surface energy and surface stress.

Therefore, if one knows the functional dependence of q on atomic separation or its derivatives, the size-and-shape dependence of the quantity Q of a nanometric system is then definite. This means that one can design materials composed of nanosolids with desired functions based on the prediction, simply by tuning the shape and size of the solid. Typical samples will be analysed in the next section.

3. Analysis

3.1. Lattice contraction

For a freestanding nanosolid the lattice constants are often measured to contract, while for a nanosolid embedded in a matrix of different materials or passivated chemically the lattice constants may expand. For example, oxygen chemisorption could expand the first metallic interlayer by up to 10–25% though the oxygen–metal bond contracts [13, 27, 30]. Yu *et al* [31] found that the mean lattice constants of Sn and Bi nano-particles contract with decreasing particle size. The contraction of the c-axis lattice is more significant than that of the a-axis lattice. By examining the bond length between neighbouring atoms of Ag, Cu, Ni and Fe in different structures, Kara and Rahman [32] found that these elements follow a strong bond-order–bond-length correlation [20]. Because of this correlation, the bond length between an atom and its neighbours would decrease with decreasing coordination. Thus the lengths of the dimer bond (2.53, 2.22, 2.15 and 2.02 Å, for Ag, Cu, Ni and Fe, respectively [20]), are shorter than the nearest-neighbouring distance in their respective bulk values by 12.5% for Ag, 13.2% for Cu, 13.6% for Ni and 18.6% for Fe. The pattern of dimer bond relaxation coincides with the surface relaxations of the top layer atoms for these elemental solids with various orientations.

Figure 2(a) shows the consistency between predictions and measurements of the size dependence of lattice contraction of Ni, Cu and Ag nanosolids based on the relation [10]

$$\frac{\Delta d(D)}{d(\infty)} = \sum_{i \leqslant 3} \gamma_i (c_i - 1) \tag{6}$$

and the relation of equation (1) with the effective CN of $z_1 \sim 4$ ($c_1 = 0.90, 0.88$), $z_2 = 6$($c_2 = 0.97, 0.96$) which covers the contribution from high order CN and the charge density. Agreement for the size dependent lattice strain of Bi and Sn has been given in [10].

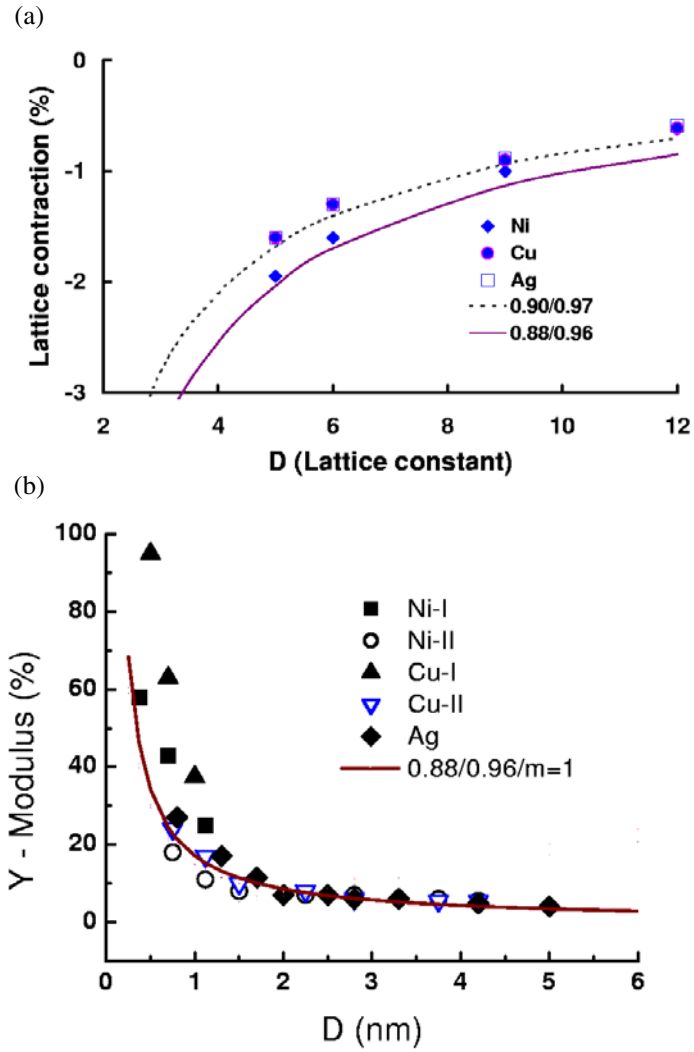

Figure 2. Agreement between predictions and observations on the size dependence of (a) the mean lattice contraction of Ni, Cu and Ag nanoparticles [33] and (b) the Young's modulus of Ni (I [38], II [39]), Cu (I [38], II [39]) and Ag [39] thin films. Agreement is reached by taking $z_1 = 4$ ($c_1 = 0.88, 0.9$), $z_2 = 6$ ($c_2 = 0.96, 0.97$) and $m = 1$.

3.2. Surface stress and nanobeam mechanics

3.2.1. Surface stress. Surface stress links the microscopic bonding configuration at an interfacial region with its macroscopic properties [33, 34]. It plays a central role in the thermodynamics and acoustics of solid surfaces. During the last decade, increasing interest has been paid to processes that are strongly influenced by surface stress effects such as reconstruction, interfacial mixing, segregation and self-organization at solid surfaces. However, detailed knowledge about the underlying atomistic processes of surface stress is yet lacking. The fact of surface bond contraction and its effect on the bond energy may provide us with the possible physical origin for surface and interface stress formation, besides the surface stress caused by chemical reaction.

The Young's modulus (E) and the stress (P) at a surface can be expressed as functions of the binding energy, E_B, volume, $v \propto d^3$, and atomic distance, d. E and P share the same dimension [22]:

$$\begin{aligned} P &= -\frac{\partial u(r)}{\partial v}\bigg|_{r=d} \propto E_B/d^3; \\ E &= v\frac{\partial P}{\partial v} = v\frac{\partial^2 u(r)}{\partial v^2}\bigg|_{r=d} \propto E_B/d^3. \end{aligned} \tag{7}$$

The relative change of the local E_i and P_i shares a common dimensionless form:

$$\frac{\Delta E_i}{E} = \frac{\Delta P_i}{P} = \frac{\Delta E_B(d_i)}{\varepsilon} - 3\frac{\Delta d_i}{d} = c_i^{-m} - 1 - 3(c_i - 1) = c_i^{-m} - 3c_i + 2 > 0. \tag{8}$$

This relation implies that both E and P at a surface should be higher than their bulk values and the changes of both E and P follow the same trends because of the bond-OLS correlation.

An examination of the hardness (also stress) and the Young's modulus of a TiCrN surface using nanoindentation [22] revealed that the surface hardness of the TiCrN thin film (2 μm thick) is 200% higher than its bulk value. Similar results have been observed by Shi *et al* [35] from amorphous carbon thin films and by Caceres *et al* [36] from an AlGaN surface. Solving equation (8) with the measured value of $\Delta P/P = 1$ gives rise to the c_i value 0.883, that corresponds to $m = 4$ [22]. Figure 2(b) shows the thickness dependence of the Young's modulus of Ni (I [37], II [38]), Cu (I [37], II [38]) and Ag [38] thin films. Calculation was based on a weighted sum over the top two atomic layers with the data $z_1 = 4$, $z_2 = 6$ and $m = 1$ for the pure metals. At the thinner end of the limit, $D = 0.5$ nm (two atomic layers), the Young's modulus of Cu is 100% higher than the bulk value, which agrees with that detected from the TiCrN surface [22].

3.2.2. Nanobeam mechanics. According to equations (3) and (6), one can derive that, for a solid nanorod, $\sum_{i=1}^{\leqslant 3} \gamma_i \propto 1/k < 1$. This means that the overall $\Delta Q/Q$ of a solid nanorod varies approximately with the inverse radius ($1/k$) of the rod and the value should be higher than the corresponding bulk value. However, for a hollow nanotube with a limited number of walls, $\sum_{i=1}^{\leqslant 3} \gamma_i \approx 1$; $\Delta Q/Q$ arises from all the atoms at the sites with strong CN reduction. $\Delta Q/Q$ approaches a constant value depending less on the diameter of the tube. $Q(D)$ is much greater than any bulk value including the rod of the same material as $Q(D)$ arises from atoms that are all at the surface region. These predictions agree well with the discovery of Wong *et al* [39] on the radius dependence of the Young's modulus of SiC nanorods and multi-walled carbon nanotubes. By using atomic force microscopy, Wong *et al* found that the multi-walled carbon nanotubes are about twice as stiff as the SiC nanorods and that the strengths of the SiC nanorods are substantially greater than those found for large SiC structures (600 GPa). The Young's modulus is 610 and 660 GPa for SiC rods of 23.0 and 21.5 nm across, respectively. For hollow carbon tubes, the modulus is 1.28 ± 0.59 TPa with no apparent dependence on the diameter of the nanotubes.

Findings of the surface stress enhancement, thickness and radius dependence of the Young's modulus of the thin Ni, Cu and Ag metal plates and the C and SiC nanobeams provide direct evidence for the essentiality of the bond-OLS correlation premise and its consequences on the mechanical strength of a surface and nanobeams. Therefore, the surface stress and its corresponding properties result from the spontaneous bond relaxation at the surface, rather than the inverse sequence that the surface stress compresses the surface bond to contract.

3.3. Critical temperature for melting and phase transition

It is understandable that the melting or phase transition of a solid requires heat energy close to the cohesive energy of this system containing numerous atoms. This fact allows the size dependence of the critical temperature for phase transition and melting of a nanosolid to be formulated as follows.

It is known that the total energy of a single bond is composed of two parts:

$$E_{total}(r,T) = E_B(r) + E_V(T) = \begin{cases} 0, & \text{evaporation} \\ E_C & \text{liquidization, or phase transition.} \end{cases} \tag{9}$$

The physical ground for the model is that if one wishes to loosen an atom of the solid thermally (melting or phase transition), one must supply sufficient thermal energy to overcome the cohesion of the specific atom to its surroundings. The thermal energy required to loosen one bond is the separation between E_C and the minimal bond energy E_B, as illustrated in figure 1(b). If the thermal vibration energy $E_V(T)$ is sufficiently large, all the bonds of the specific atom will break and the atoms will escape from the bulk. At the evaporating point of any kind of solid, $E_{total} = 0$; at the critical point of melting or phase transition, $E_{total} = E_C$. E_C may vary from material to material and from process to process but for a specific material and a specific process (melting or phase transition), the energy difference between E_C and $E_{eva}(=0)$ should be identical. This means that the principle of thermal equilibrium holds for the entire solid disregarding its size. Therefore, it is not surprising that the temperature is always the same throughout the solid while the critical temperature varies from site to site if the sample contains atoms with different CNs, which is the case of atoms at the surface or at sites surrounding voids or stacking defects. This mechanism may explain why the latent energy of fusion was measured as a broad hump rather than a sharp peak [40]. The idea of identical E_C for all the bonds in a solid supports the model of random fluctuation melting [41] because the energy required to break one bond (separation between E_B and E_C) and hence the energy needed to melt an individual atom with different CN may be different.

If the thermal energy required to loose a single bond of an atom in the ith atomic layer and that for a bulk atom are $E_{VC,i}$ and $E_{VC,b}$, respectively, the difference between the thermal energy required to loose the corresponding atoms will be $z_i E_{VC,i} - z_b E_{VC,b}$, if all the z_i and z_b bonds are identical in nature. z_i and z_b are the effective CNs of the corresponding atoms. Hence, the total thermal energy at the critical point of a solid with N atoms is given as

$$\begin{aligned} E_{VC}(D) &= Nz_b E_{VC,b} + \sum_{i\leqslant 3} N_i(z_i E_{VC,i} - z_b E_{VC,b}) \\ &= E_{VC}(\infty) + \sum_{i\leqslant 3} N_i z_b E_{VC,b}(z_{ib}E_{VC,ib} - 1) \end{aligned} \tag{10}$$

where $z_{ib} = z_i/z_b$ and $E_{VC,ib} = E_{VC,i}/E_{VC,b} = c_i^{-m}$ are the normalized CN and the normalized critical thermal energy, respectively. Here we quantize statistically N_S or the surface 'shell' of unknown thickness involved in other models as the contribution of individual atomic layers. In dealing with a nanosolid, one has to consider bond by bond and atom by atom. The statistic quatitization never means isolating thermally one bond or one atom from another, as the thermal equilibrium holds for the entire solid disregarding its size. Therefore, the relative change of $E_{VC}(D)$, for melting or transiting a nanosolid from one phase to another, to $E_{VC}(\infty)$ for the solid without bond relaxation is

$$\frac{\Delta E_{VC}(D)}{E_{VC}(\infty)} = \frac{E_{VC}(D) - E_{VC}(\infty)}{E_{VC}(\infty)} = \sum_{i\leqslant 3} \gamma_i(z_{ib}c_i^{-m} - 1). \tag{11}$$

On the other hand, integrating the specific heat from zero to the critical point, one will have

$$\frac{\Delta E_{VC}(D)}{E_{VC}(\infty)} = \frac{\int_0^{T_C(D)} C_p(D,T)\,\mathrm{d}T}{\int_0^{T_C(\infty)} C_p(\infty,T)\,\mathrm{d}T} - 1 \cong \frac{\Delta T_C(D)}{\Delta T_C(\infty)}. \tag{12}$$

It has been found reasonable to take $C_p(D,T) \cong C_p(\infty,T) \cong$ constant in the entire temperature range [9] for the first order approximation though negligible errors may exist because the Debye temperature and hence the specific heat C_P is size and temperature dependent [42–44]. Therefore, combining equations (11) and (12) leads to

$$\frac{\Delta T_C(D)}{T_C(\infty)} = \frac{\Delta E_{VC}(D)}{E_{VC}(\infty)} = \sum_{i\leqslant 3} \gamma_i (z_{ib} c_i^{-m} - 1). \tag{13}$$

T_C can be any critical temperature for events such as phase transition, liquidation or evaporation. Equation (13) indicates that $\Delta T_C(D)$ originates from the difference between the cohesive energy of an atom at the surface and that inside the bulk, $z_{ib}c_i^{-m} - 1$. The approach favours the atomistic model of Shi [45] and Jiang [46, 47] who ascribed the melting behaviour of a nanosolid to the difference in the amplitude of atomic vibration at surface and bulk as $(-[(\sigma_s/\sigma_b)^2 - 1])$. The lattice-vibration model has been applied well to the size-dependent melting of compounds [46], metals [48], nanotubes [49], polymers [50], glasses [51], inert gases [52], ice [53] and semiconductors [54]. In conjunction with the model of Shi and Jiang, the current bond-OLS correlation premise could deepen the insight into the physical origin and the general trends of the melting and phase transition behaviour of a nanometric solid. It is seen that in the present premise the difference of atomic E_{Coh}, $\Delta E_{Coh}/E_{Coh} = (z_{ib}c_i^{-m} - 1)$, claims the origin for the change, compared with the lattice-vibration premise in which $-[(\sigma_s/\sigma_b)^2 - 1]$ governs. It is understandable that the amplitude of atomic vibration is determined by the cohesive energy of the specific atom. At a free surface, the atomic E_{Coh} is lower than that of the bulk value and the vibration amplitude of an atom at the free surface is larger than that inside the bulk at the same temperature. This bond-OLS correlation also supports the liquid-shell model [55–57] because the lowered surface atomic E_{Coh} allows the atom in the relaxed region to be liquidized more easily than the bulk atom with higher E_{Coh}. At the lower end of the size limit, the homogeneous melting mechanism [58, 59] dominates. For a nanosolid embedded in a matrix, the atomic cohesive energy at the interface may rise because of the enhanced bond energy and slightly changed CN. Therefore, melting a nanosolid embedded in a matrix should be harder [45]. Figures 3(a) and (b) show the consistency between predictions and measurements of the size dependence of T_C for ferromagnetic Ni [60, 61] thin films ($T_C(\infty) = 670$ K) and the melting point, T_m, for an Au thin film ($T_m(\infty) = 1593$ K) on C substrate [62], with the data $z_{1b} = 1/3$ ($c_1 = 0.88$), $z_{2b} = 1/2$ ($c_2 = 0.96$) and $m = 1$. Comparison between predictions of different dimensionality with observations indicates that the thinnest Au film tends to be spherical-like—island mode of growth.

3.4. Phonon and photon emission

3.4.1. Surface phonon. The frequency of atomic vibration, $\omega \propto f_k^{1/2}$, depends on the force constant that can be derived from the binding energy at equilibrium atomic separation:

$$f_k = \left.\frac{\partial^2 u(r)}{\partial r^2}\right|_{r=d} \propto \frac{\epsilon}{d^2}. \tag{14}$$

The frequency change of the atomic vibration due to the bond-OLS correlation is given as

$$\frac{\Delta\omega(D)}{\omega(\infty)} = \sum_{i\leqslant 3} \gamma_i \left(\frac{\Delta f_k}{2 f_k}\right) = \sum_{i\leqslant 3} \gamma_i \left[\frac{1}{2}(c_i^{-m} - 1) + (c_i - 1)\right]. \tag{15}$$

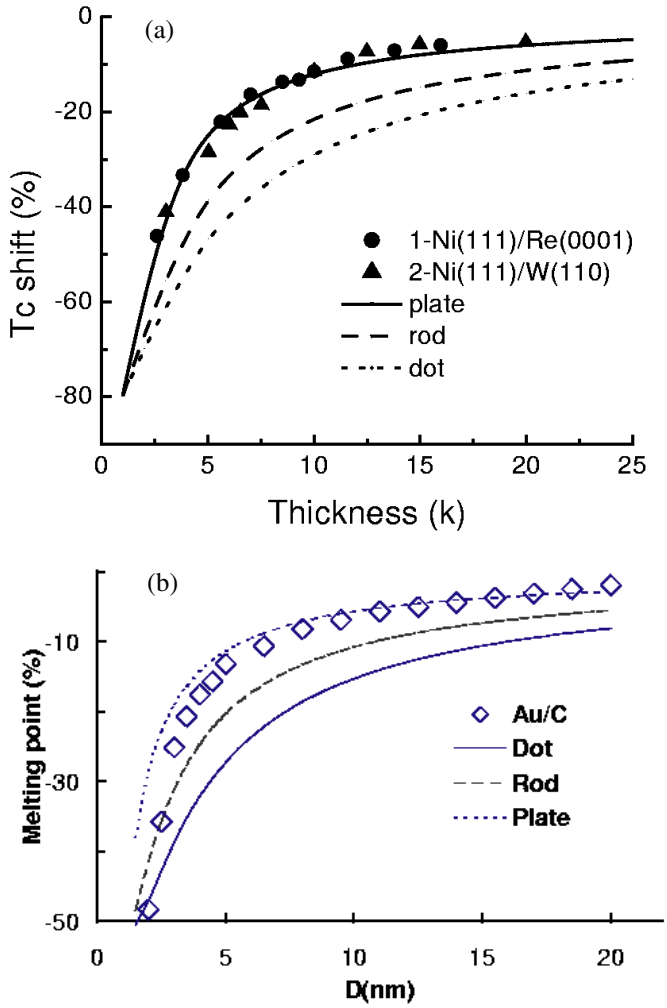

Figure 3. Agreement between predictions and measurements on the size dependence of (a) the Curie temperature, T_C, for Ni [57] and (b) the melting point, T_m, for Au on C [58] thin films. Agreement is reached with the same data of $z_{1b} = 1/3$ ($c_1 = 0.88$), $z_{2b} = 1/2$ ($c_2 = 0.96$) and $m = 1$.

For a nanosolid, the mean frequency change depends on the binding energy density and the bond length (see equation (14)) and the portion of surface atoms, γ_i. Agreement between prediction and observation of the size-dependent Raman shift (140 cm^{-1} peak) of TiO_2 nanosolid [63] is obtained by taking $z_{ib} = 1/3$ and $1/2$, and $m = 4$, as shown in figure 4(a).

3.4.2. Photon emission and photon absorption. The wavelength of a photon emitted from, or absorbed by, a semiconductor depends on the bandgap of the solid. The band gap, and also the core-level shift, is a function of the Hamiltonian of the solid [23]:

$$\hat{H}(D) = \hat{H}(\infty) + \hat{H}'(D) = -\frac{\hbar^2\nabla^2}{2m} + V_{atom}(r) + V_{cry}(r + R_C)[1 + \Delta(D)]$$
$$\hat{H}'(D) = V_{cry}(r + R_C)\Delta(D). \tag{16}$$

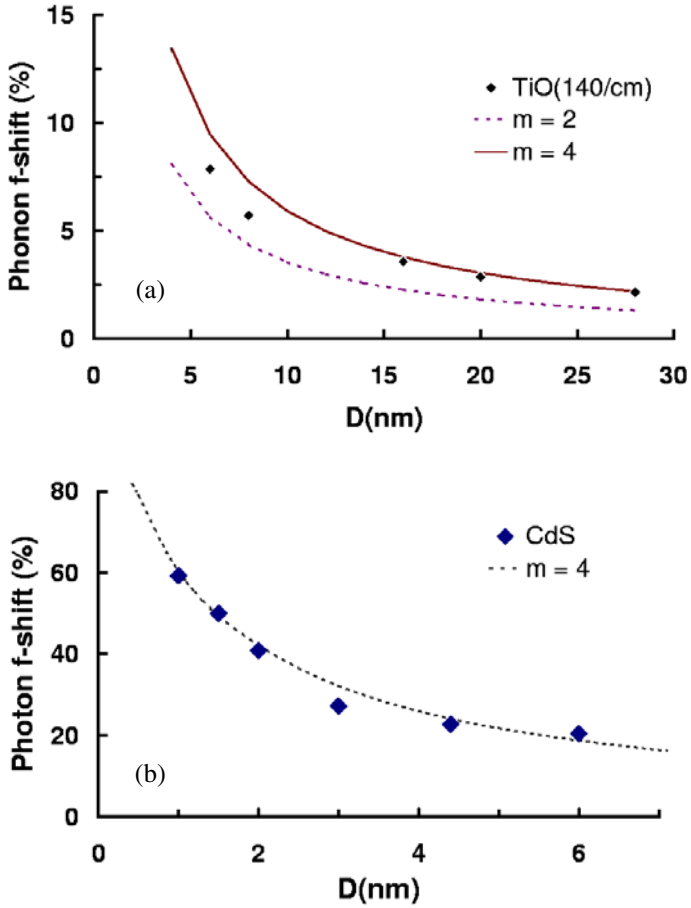

Figure 4. Agreement between predictions and measurements of the size dependence of (a) Raman frequency shift ($\omega_0 = 140$ cm^{-1}) of TiO_2 [59], and (b) the blue-shift in photoluminescence of CdS [28]. Agreement is reached at $z_{ib} = 1/3$ ($z_{1b} = 0.88$), $z_{2b} = 1/2$ ($c_2 = 0.96$) and $m = 4$.

$V_{atom}(r)$ is the intra-atomic trapping potential of an isolated atom, which determines the discrete energy levels of the atom. $V_{cry}(r + R_C)$ is the crystal potential for an extended solid, that sums the inter-atomic binding energy over the solid, which evolves the single energy level of an isolated atom to the energy band when a solid forms with numerous atoms. Without the crystal potential, no solid could form. $\hat{H}'(D)$ is the contribution of surface relaxation to the crystal field of an extended solid. R_C is the lattice constant. $\Delta(D)$, being independent of the particular form of the interatomic potential, is given by [24]

$$\Delta(D) = \sum_{i\leqslant 3} \gamma_i \frac{\Delta v(d_i)}{v(d)} + \delta(D) = \sum_{i\leqslant 3} \gamma_i (c_i^{-m} - 1) + \delta(D) \tag{17}$$

where $\delta(D)$ describes the contribution of intercluster interaction, which becomes insignificant with increasing particle size D. For a single particle, $\delta(D) = 0$. The bond-OLS-induced bandgap expansion and core-level shift are derived as

$$\frac{\Delta E_g}{E_g} = \frac{\Delta E_{core}}{E_{core}} = \Delta(D). \tag{18}$$

Intensive discussion on the modified Hamiltonian and its effect on the entire band structure (bandgap, core-level shift, band tails and band width) of SiO, CuO, III–V and II–VI nanosolids have formed the subject of [23]. Progress reported therewith showed consistency between predictions and observations in the band characteristics of nanosolids. Figure 4(b) compares the observed with the predicted size-dependent photoluminescence frequency of nanometric CdS [64] with the data of $z_{1b} = 1/3$ ($c_1 = 0.88$), $z_{2b} = 1/2$ ($c_2 = 0.96$) and $m = 4$. Near the lower end of the size limit, z_{1b} is around one-quarter due to the increased surface curvature.

3.5. Other applications

The bond-OLS correlation has also been incorporated into other observations. For example, properties pertaining to the crystal field such as the dielectric susceptibility $\chi(\varepsilon_r = \chi + 1$, $\chi \propto E_g^{-2}$ [65]) and the saturation magnetization M_s [66] of a nanosolid will change accordingly and they are detectable as mean values over the entire solid. Such relative changes can be expressed in a dimensionless form:

$$-\frac{1}{2}\frac{\Delta\chi}{\chi} = \frac{\Delta M_s}{M_s} = \Delta(D). \tag{19}$$

In comparison with the Penn model [67] and its modified forms [68, 69], simulation of the size-dependent $\Delta\chi/\chi$ for a semiconductor nanosolid and its consequence on the photon absorption coefficient has been reported in [24]. Predictions also agree with the XPS measurements of the core-band shift of SnO_2 and Ta_2O_5 [70] as well as the O–Cu [71], CdS[72] and ZnS [73] nanoparticles. The surface stress enhancement has an influence on the Gibbs free energy and hence the relaxation and transition of the ferroelectric and pyroelectric properties of nanometric PZT oxides, as reported in [74, 75].

It is our opinion that any size-induced change of a physical quantity should be readily defined with the known bulk value (as a reference) of the specific quantity and its functional dependence on the atomic distance or its derivatives. This premise is purely a geometrical effect at the surface that is independent of the nature of the bond. As a matter of fact, the binding energy at equilibrium atomic separation is independent of the particular forms of the pair-wise potential which is a resultant of different order CNs and the effect of charge distribution—no matter whether the delocalized conduction electrons for metals or the localized electrons for compounds. As demonstrated, the different m values for metals and for compounds may reflect the chemical contribution.

4. Conclusion

Based on the Goldschmidt premise a bond-OLS correlation mechanism has been developed, which has enabled us to unify the shape-and-size dependence of a nanosolid for a number of properties and to link them to the effect of CN imperfection at a surface and its effect on the bond energy.

The premise is indeed very simple and straightforward involving no assumptions or freely adjustable variables. The only parameter used is m, that varies with the nature of the bond involved. For elemental solid, $m = 1$; for compounds or alloys, $m = 4$. As demonstrated in this work and earlier reports, this bond-OLS correlation premise has led to consistent understanding of the size dependence of a considerable number of properties of nanosolids. These properties include the mean lattice strain, surface stress and Young's modulus, dielectrics (photon absorption), bandgap (blue-shift in photoluminescence), core-level shift (chemical reactivity), critical temperature for melting (supercooling and superheating) and phase transition (magnetic

and dielectric). For the case of lattice expansion, this premise is also valid (letting $c_i > 1$, $m < 0$) unless the lattice relaxation is non-spontaneous. It should be understandable that a spontaneous process is always accompanied by minimization of the system energy.

The significance of this premise lies not in the simulation of the observations; rather, it provides guideline for designing nonmaterials or devices with desired functions based on the predicted shape-and-size dependence. It is expected that all the traditional characteristic constants relating to the atomic distance, whether direct or indirect, could be predictably tunable by controlling the physical shape and size of the system, if the functional dependence of these quantities is established, according to the current premise.

References

[1] Canham L T 1990 *Appl. Phys. Lett.* **57** 1046
[2] Stoneham A M 1999 *J. Phys.: Condens. Matter* **11** 8351
[3] Koch F, Petrova-Koch V, Muschik T, Nikolov A and Gavrilenko V 1993 *Microcrystalline Semiconductors: Materials Science and Devices* vol 283 (Pittsburgh, PA: Materials Research Society) p 197
[4] Qin G G and Jia Y Q 1993 *Solid State Commun.* **86** 559
[5] Pauling L 1947 *J. Am. Chem. Soc.* **69** 542
[6] Goldschmidt V M 1927 *Ber. Deutsch. Chem. Ges.* **60** 1270
[7] Sun C Q and Bai C L 1997 *J. Phys. Chem. Solids* **58** 903
[8] Two sequential review reports:
Sun C Q 2001 *Surf. Rev. Lett.* **8** 367
Sun C Q 2001 *Surf. Rev. Lett.* **8** 703
[9] Sinnott M J 1963 *The Solid State for Engineers* (New York: Wiley)
[10] Sun C Q 1999 *J. Phys.: Condens. Matter* **11** 4801
[11] Halicioglu T 1991 *Surf. Sci.* **259** L714
[12] Baraldi G, Silvano L and Comelli G 2001 *Phys. Rev.* B **63** 115410
[13] Over H, Kleinle G, Ertl G, Moritz W, Ernst K H, Wohlgemuth H, Christmann K and Schwarz E 1991 *Surf. Sci.* **254** L469
[14] Davis H L and Zehner D M 1980 *J. Vac. Sci. Technol.* **17** 190
[15] Qian X and Hübner W 1999 *Phys. Rev.* B **60** 16 192
[16] Geng W T, Freeman A J and Wu R Q 2001 *Phys. Rev.* B **63** 064427
[17] Geng W T, Kim M and Freeman A J 2001 *Phys. Rev.* B **63** 245401
[18] Batra I P 1985 *J. Vac. Sci. Technol.* A **33** 1603
[19] Bahn S R and Jaconsen K W 2001 *Phys. Rev. Lett.* **87** 266101
[20] Feibelman P J 1996 *Phys. Rev.* B **53** 13 740
[21] Sun C Q 1997 *Vacuum* **48** 535
[22] Sun C Q, Tay B K, Lau S P, Sun X W, Zeng X T, Bai H, Liu H, Liu Z H and Jiang E Y 2001 *J. Appl. Phys.* **90** 2615
[23] Sun C Q, Chen T P, Tay B K, Li S, Huang H, Zhang Y B, Pan L K, Lau S P and Sun X W 2001 *J. Phys. D: Appl. Phys.* **34** 3470
[24] Zhong W H, Sun C Q, Tay B K, Li S, Bai H L and Jiang E Y 2002 *J. Phys.: Condens. Matter* **14** L399
[25] Sun C Q, Sun X W, Tay B K, Lau S P, Huang H and Li S 2001 *J. Phys. D: Appl. Phys.* **34** 2359
[26] Pauling L 1939 *The Nature of the Chemical Bond* (3rd edn 1960) (New York: Cornell University Press)
[27] Sun C Q 1997 *Vacuum* **48** 865
[28] Sun C Q and Bai C L 1997 *J. Phys.: Condens. Matter* **9** 5823
[29] Tománek D, Mukherjee S and Bennemann K H 1983 *Phys. Rev.* B **28** 665
[30] Jennings P and Sun C Q 1992 *Surface Analysis Methods in Materials Science* (4th edn 2002) ed D J O'Connor, B A Sexton and R C Smart (Berlin: Springer)
[31] Yu X F, Liu X, Zhang K and Hu Z Q 1999 *J. Phys.: Condens. Matter* **11** 937
[32] Kara A and Rahman T S 1998 *Phys. Rev. Lett.* **81** 1453
[33] Ibach H 1997 *Surf. Sci. Rep.* **29** 193
[34] Haiss W 2001 *Rep. Prog. Phys.* **64** 591
[35] Shi X, Tay B K, Flynn D L and Sun Z 1997 *Mater. Res. Soc. Symp. Proc.* **436** 293
[36] Caceres D, Vergara I, Gonzalez R, Monroy E, Calle F, Munoz E and Omnes F 1999 *J. Appl. Phys.* **86** 6773
[37] Dodson B W 1988 *Phys. Rev. Lett.* **60** 2288

[38] Streitz F H, Cammarata R C and Sieradzki K 1994 *Phys. Rev.* B **49** 10 699
[39] Wong E W, Sheehan P E and Lieber C M 1997 *Science* **277** 1971
[40] Lai S L, Guo J Y, Petrova V, Ramanath G and Allen L H 1996 *Phys. Rev. Lett.* **77** 99
[41] Vekhter B and Berry R S 1997 *J. Chem. Phys.* **106** 6456
[42] Jiang Q, Tong H Y, Hsu D T, Okuyama K and Shi F G 1998 *Thin Solid Films* **31** 2357
[43] Lu K 1996 *Mater. Sci. Eng.* **R16** 161
[44] Ding X Z and Liu X H 1996 *Phys. Status Solidi* a **158** 433
[45] Shi F G 1994 *J. Mater. Res.* **9** 1307
[46] Jiang Q, Zhang Z and Li J C 2000 *Chem. Phys. Lett.* **322** 549
[47] Zhang Z, Li J C and Jiang Q 2000 *J. Phys. D: Appl. Phys.* **33** 2653
[48] Jiang Q, Liang L H and Li J C 2001 *J. Phys.: Condens. Matter* **13** 565
[49] Jiang Q, Aya N and Shi F G 1997 *Appl. Phys.* A **64** 627
[50] Jiang Q, Shi H X and Zhao M 1999 *J. Chem. Phys.* **111** 2176
[51] Jiang Q, Shi H X and Li J C 1999 *Thin Solid Films* **354** 283
[52] Wen Z, Zhao M and Jiang Q 2000 *J. Phys.: Condens. Matter* **12** 8819
[53] Jiang Q, Liang L H and Zhao M 2001 *J. Phys.: Condens. Matter* **13** L397
[54] Zhang Z, Zhao M and Jiang Q 2001 *Semicond. Sci. Technol.* **16** L33
[55] Ubbelohde A R 1978 *The Molten State of Matter* (New York: Wiley)
[56] Wronski C R M 1967 *J. Appl. Phys.* **18** 1731
[57] Hanszen K J 1960 *Z. Phys.* **157** 523
[58] Buffat P and Borel J-P 1976 *Phys. Rev.* **13** 2287
[59] Pawlow P 1909 *Z. Phys. Chem. (Munich)* **65** 1
[60] Li Y and Baberschke K 1992 *Phys. Rev. Lett.* **68** 1208
[61] Bergholz R and Gradmann U 1984 *J. Magn. Magn. Mater.* **45** 389
[62] Buffat P and Borel J-P 1976 *Phys. Rev.* **13** 2287
[63] Zhang W F, He Y L, Zhang M S, Yin Z and Chen Q 2000 *J. Phys. D: Appl. Phys.* **33** 912
[64] Wang Y and Herron N 1990 *Phys. Rev.* B **42** 7253
[65] Tsu R, Babic D and Loriatti L Jr 1997 *J. Appl. Phys.* **82** 1327
[66] Shi J, Gider S, Babcock K and Awschalom D D 1996 *Science* **271** 937
[67] Penn D R 1962 *Phys. Rev.* **128** 2093
[68] Wang L W and Zunger A 1996 *Phys. Rev.* B **53** 9579
[69] Allan G, Delerue C, Lannoo M and Martin E 1995 *Phys. Rev.* B **52** 11 982
[70] Schmeißer D, Böhme O, Yfantis A, Heller T, Batchelor D R, Lundstrom I and Spetz A L 1999 *Phys. Rev. Lett.* **83** 380
[71] Borgohain K, Singh J B, Rao M V R, Shripathi T and Mahamuni S 2000 *Phys. Rev.* B **61** 11 093
[72] Nanda J, Kuruvilla A and Sarma D D 1999 *Phys. Rev.* B **59** 7473
[73] Nanda J and Sarma D D 2001 *J. Appl. Phys.* **90** 2504
[74] Huang H, Sun C Q, Zhang T S and Hing P 2001 *Phys. Rev.* B **63** 184112
[75] Huang H, Sun C Q and Hing P 2000 *J. Phys.: Condens. Matter* **12** L127